Fluorescence resonance energy transfer on single living cells

Application to binding of monovalent haptens to cell-bound immunoglobulin E

Ulrich Kubitscheck,*§ Martin Kircheis,* Reinhard Schweitzer-Stenner,* Wolfgang Dreybrodt,* Thomas M. Jovin,‡ and Israel Pecht§

*Institute for Experimental Physics, University of Bremen, 2800 Bremen 33; ‡Department of Molecular Biology, Max Planck Institute of Biophysical Chemistry, D-3400 Göttingen, Germany; and §Department of Chemical Immunology, The Weizmann Institute of Science, Rehovot 76100, Israel

ABSTRACT We have determined the specific binding of 2,4-dinitrophenyl (DNP)-haptens to two different monoclonal immunoglobulin (IgE) molecules bound to Fc_ϵ-receptors on the cell surface of single, living rat basophilic leukemia cells subclone 2H3 cells. The measurements were performed at 4°, 15°, and 25°C using a recently developed technique that permits the quantitative determination of fluorescence resonance energy transfer between two fluorophores on single cells in a microscope from the photobleaching kinetics of the donor fluorophore. We introduce here a method for performing binding studies on individual attached cells. At 25°C, the titration studies yielded equilibrium binding constants K_{int} of $9 \cdot 10^8$, $8 \cdot 10^8$, and $8 \cdot 10^7$ M^{-1} for the monovalent haptens *N*-2,4-DNP-ε-amino-*n*-caproic acid, *N*ε-2,4-DNP-L-lysine, and *N*-2,4-DNP-γ-amino-*n*-butyric acid, respectively. Our data indicate that the affinity constants for the first two haptens binding to IgE on adherent cells are 4 to 11 times larger than that of the corresponding values obtained by fluorescence quenching experiments with the same haptens and IgE molecules either in solution or bound to cells in suspension.

INTRODUCTION

In mast cells and basophils aggregation of the membrane receptor for immunoglobulin E (IgE; type I Fc_ϵ-receptor ($Fc_\epsilon RI$))[1] initiates a cascade of reactions culminating in exocytosis and secretion of granula containing mediators of inflammation (1). This system is regarded as a model for studying the initial step of receptor-mediated signaling across biological membranes.

It is not clear, however, what physical and steric conditions must be met by the receptor aggregates to trigger the cellular response (1, 2). A physical definition in terms of the quantity, lifetime, geometry, and flexibility of the molecular complex inducing cell activation requires further study. One approach is to investigate the properties and effects of distinct receptor aggregates involving defined haptenic ligands specific for the combining sites of monoclonal IgE, the physiological mediator of receptor aggregation. Divalent haptens of known length and flexibility have been used as cross-linking reagents in experiments performed on IgE in solution (3) and bound to the surface of cells in suspension (4, 5).

The very first step of the cross-linking process is the recognition and binding of hapten by the IgE. Our experiments center on this first binding equilibrium. We examined whether the anchoring of an IgE to the Fc_ϵ-receptor affects the affinity of its paratopes to binding haptens. The answer to this question reflects on antibody function in general and provides a comparison of binding experiments of IgE in solution to those of receptor-bound IgE.

Recently a new method was introduced (6, 7) to measure fluorescence energy transfer between proteins or other molecules on single cells in a microscope. Since the energy transfer efficiency is dependent on the inverse sixth power of the distance between the donor and acceptor, information on the structure of appropriately labeled components can be obtained in vivo. By distance measurements between different proteins the spatial arrangement of, or functional linkages between, the molecules in question may be deduced.

The new method uses the photobleaching of the fluorescence donor to calculate the efficiency of energy transfer to the acceptor. The validity of this approach was first demonstrated in a system where fluorescently labeled lectins were specifically bound to surface membrane glycoproteins and glycolipids on mammalian cells (7). This method was compared with the determination of energy transfer by sensitized acceptor emission in a microscope. Although both methods yield the same results, the photobleaching method offers distinct advantages in that complex corrections associated with the determination of energy transfer by combined donor and sensitized acceptor emissions are avoided.

We have now extended application of this technique to binding studies performed on single living cells. This provides a new way to measure affinity constants that

Address correspondence to Dr. Schweitzer-Stenner.

[1] *Abbreviations used in this paper:* BSA: bovine serum albumin; DNP: 2,4-dinitrophenyl; DNP-but: *N*-2,4-DNP-γ-amino-*n*-butyric acid; DNP-cap: *N*-2,4-DNP-ε-amino-*n*-caproic acid; DNP-lys: N_ϵ-2,4-DNP-L-lysine; IgE: Immunoglobulin E; PBS: Phosphate buffered saline; RBL-2H3: rat basophilic leukemia cells subclone 2H3.

0006-3495/91/08/307/12 $2.00

requires for each titration curve an extremely small number of cells. We demonstrate that binding curves can be obtained from energy transfer data for appropriately labeled donor and acceptor molecules. Fluorescein-labeled, 2,4-dinitrophenyl (DNP)-specific monoclonal IgE H1-26.82 (8) and SPE-7 (9) served as the energy donor and monovalent DNP-haptens with different side chains as energy acceptors (4). Monitoring of the binding process on the cell surface by energy transfer is feasible because fluorescein is excited in the visible part of the spectrum, where only a limited cellular autofluorescence background is elicited. We determined the equilibrium binding constants of three different haptens to monoclonal IgE bound to its type I Fc_ϵ-receptor on the surface of live rat basophilic leukemia cells (RBL-2H3). The data at 4°, 15°, and 25°C are compared with those of binding experiments performed with the same IgE free in solution and bound to cells in suspension.

THEORETICAL BACKGROUND

Resonance fluorescence energy transfer

In a fluorescence process light of intensity I_0 excites the fluorophore (donor) from the ground state D_0 to a state D^* at a rate k_{ex}. D^* decays with a rate k_d by radiative and nonradiative processes. Introducing a suitable acceptor A opens a new decay path by nonradiative energy transfer with rate k_{et} (Fig. 1). Förster's theory (10) shows that for a single donor-acceptor pair k_{et} is given by:

$$k_{et} = k_d \cdot (R_0/R)^6, \quad (1)$$

where R_0 is the Förster distance corresponding to 50% energy transfer, a constant that is specific for a given donor-acceptor pair. It is dependent on the refractive index of the medium, the quantum yield of the donor in

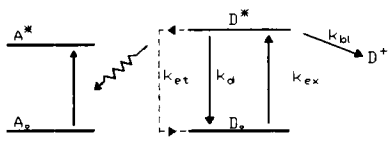

FIGURE 1 Photophysical scheme for photobleaching fluorescence energy transfer. Light of intensity I_0 transfers the donor fluorophore from the ground state D_0 to an excited state D^* with rate k_{ex}. D^* decays with a rate k_d by radiative and nonradiative processes. Introducing a suitable acceptor A opens a new path of decay with rate k_{et} by energy transfer. Each molecule in the excited state has a given probability to be destroyed by photobleaching (rate k_{bl}) and then does not further contribute to fluorescence. Thus a decay of fluorescence (photobleaching) is observed. From reference 6.

absence of energy transfer, the orientation between the transition dipole moments of the donor and acceptor molecules, respectively, and the overlap integral of the donor emission and acceptor absorption spectra. The energy transfer efficiency E is defined by:

$$E = k_{et}/(k_d + k_{et}) = 1 - \tau_e'/\tau_e, \quad (2)$$

where $\tau_e' = 1/(k_d + k_{et})$ and $\tau_e = 1/k_d$ are the fluorescence lifetimes of the excited state D^* with and without energy transfer, respectively. They usually lie in the range of nanoseconds.

Determination of energy transfer by photobleaching

Each molecule in the excited state also has a given probability (rate k_{bl}) to decompose by photochemical processes (6, 7). Thus the residual fraction of original molecules contributing to fluorescence $g_{tot}(t)$ decays according to:

$$dg_{tot}(t)/dt = d[g(t) + g^*(t)]/dt = -g^*(t) \cdot k_{bl}, \quad (3)$$

where $g^*(t)$ is the fraction of donors in the excited state D^* and $g(t)$ the fraction of donors in the ground state. A decrease in fluorescence with a time constant τ_1' is observed. τ_1' is in the range of milliseconds to minutes, depending on the excitation intensity. The calculation of the time dependence of $g^*(t)$ provides us with a relationship between the photobleaching time constants and the lifetimes of the excited state.

It is possible, in principle, to measure τ_e and τ_e' directly in the nanosecond domain and thereby determine E by Eq. 2. This measurement, however, is technically difficult, especially in the microscope. A considerable simplification can be achieved by shifting the examined time domain by up to nine orders of magnitude using the above mentioned dependence of τ_1' on τ_e', which is derived by solving the following two coupled differential equations:

$$dg(t)/dt = -k_{ex} \cdot g(t) + (k_{et} + k_d) \cdot g^*(t) \quad (4a)$$

$$dg^*(t)/dt = k_{ex} \cdot g(t) - (k_{et} + k_d + k_{bl}) \cdot g^*(t). \quad (4b)$$

The exciting light increases the occupation of the excited state, whereas fluorescence and nonradiative processes, including photobleaching (second term in Eq. 4b), lead to its depletion.

For $g^*(0) = 0$ at $t = 0$ and assuming $k_{bl} \ll k_{ex} \ll k_d$ (condition of low irradiance, see reference 11) we obtain:

$$g^*(t) \approx e^{-t/\tau 1'}(1 - e^{t/\tau 2}) \quad (5)$$

τ_1' and τ_2 can be approximated as:

$$\tau_1' \approx (k_{et} + k_d)/(k_{ex} \cdot k_{bl}) = 1/(\tau_e' \cdot k_{ex} \cdot k_{bl}) \quad (6a)$$

$$\tau_2 \approx 1/(k_{et} + k_d + k_{ex}). \quad (6b)$$

In the ideal case without photobleaching ($k_{bl} = 0$) Eq. 5 describes a fast transient rise with the time constant τ_2 due to excitation from the ground state by the incident light. A steady state is then established with a constant fluorescence intensity proportional to g^*. The transient is of no importance for the following discussion and, therefore, the second exponential is omitted in the equations below. Introduction of photobleaching ($k_{bl} > 0$) produces a slow decrease of g^* with time constant τ_1' as described by the first exponential of Eq. 5. Eq. 6a gives the photobleaching time constant τ_1' as a function of τ_e' for the case of energy transfer. In the absence of energy transfer, i.e., for $k_{et} = 0$, we get:

$$\tau_1 \approx k_d/(k_{ex}k_{bl}) = (\tau_e k_{ex} k_{bl})^{-1} < \tau_1'. \quad (7)$$

Thus, energy transfer diminishes the lifetime τ_e of a fluorophore in the excited state because it provides an alternative decay route. As a consequence, the relative population of D^*, i.e., $g^*(t)$, and the rate of photobleaching are decreased.

From Eqs. 2, 6a, and 7 it follows that E can be calculated from τ_1 and τ_1' according to:

$$E = 1 - \tau_1/\tau_1'. \quad (8)$$

The energy transfer efficiency E can be obtained by measuring the time constants τ_1 and τ_1' by photobleaching experiments.

Finally, it should be noted that basically the same formalism can be applied to all mechanisms that decrease the donor's fluorescence by deactivation of the first excited singlet state, i.e., for instance charge transfer and collisional processes.

Determination of the mole fraction of donor-acceptor-pairs by photobleaching

Energy transfer has extensively been utilized for assessing intra- and intermolecular distances. Here we use it for the determination of the fraction of bound ligand molecules as a function of the total ligand concentration. A covalent conjugate of fluorescein-IgE (monoclonal, DNP-specific) serves both as energy donor and binds the acceptor molecule. Energy transfer will only occur in the bound state because the donor-acceptor distance is too large when the acceptor is free in solution. Bound DNP is an effective acceptor for fluorescein despite an unfavorable spectral overlap. This is probably due to the close proximity of the antibody combining site to the conjugation site of fluorescein on the employed monoclonal IgE's (4).

From the equations above we see that the donor fluorescence shows an exponential photobleaching with a time constant dependent on the energy transfer efficiency. In a system consisting of donor-acceptor-pairs D-A with mole fraction α and isolated donors D with mole fraction $(1 - \alpha)$, one can use the difference between their respective photobleaching time constants to determine the mole fraction α.

The fluorescence intensity of this system can be expressed as follows:

$$F(t) = F_{da} \cdot \alpha \cdot e^{-t/\tau 1'} + F_d \cdot (1 - \alpha) e^{-t/\tau 1}, \quad (9)$$

where F_d denotes the fluorescence intensity of the free donor and $F_{da} = \tau_1' \cdot F_d$ the quenched fluorescence of the donor-acceptor pairs.

The experimental procedure entails recording the photobleaching kinetics of the system. The constants F_d, α, τ_1, and τ_1' can, in principle, be determined by fitting Eq. 9 to the data. It is well known (12), however, that it is difficult to reliably determine parameters in a theoretical expression consisting of sums of exponentials with similar magnitudes by fitting procedures. To overcome this difficulty we describe the double exponential kinetics by a single exponential with an effective time constant τ_{eff}. Indeed τ_{eff} is equal to τ_1 and τ_1' for $\alpha = 0$ and $\alpha = 1$, respectively, since in both cases only one exponential is retained in Eq. 9. Knowing τ_1 and τ_1' we can determine α from τ_{eff} by the following reasoning based upon description of the data given by Eq. 9. A monoexponential fit yields a time constant τ_{eff}, so that the corresponding variance $V(\alpha)$

$$V(\alpha) = \int_0^\infty \{[1 + \alpha(\tau_1/\tau_1' - 1)] \cdot e^{-t/\tau eff} - [\alpha \cdot \tau_1/\tau_1' \cdot e^{-t/\tau 1'} + (1 - \alpha) e^{-t/\tau 1}]\}^2 dt \quad (10)$$

is minimal for the condition $dV(\alpha)/d\alpha = 0$. By solving the integral and differentiating $V(\alpha)$ we find the following relationship between α and the bleaching time constants τ_{eff}, τ_1, and τ_1':

$$\alpha = \frac{\tau_1 - 2\{\tau_1\tau_1'/(\tau_1 + \tau_1') - \tau_{eff}\tau_1/(\tau_{eff} + \tau_1) + \tau_{eff}\tau_1'/(\tau_{eff} + \tau_1')\}}{\tau_1 - 4\tau_1\tau_1'/(\tau_1 + \tau_1') + \tau_1'}. \quad (11)$$

Fig. 2 shows α as a function of E_{eff}/E_{max}, where $E_{eff} = 1 - \tau_1/\tau_{eff}$ and $E_{max} = 1 - \tau_1/\tau_1'$, for different values of E_{max}. It is apparent from Fig. 2 that for $E_{max} < 23\%$, α is linearly dependent on the effective energy transfer efficiency E_{eff}

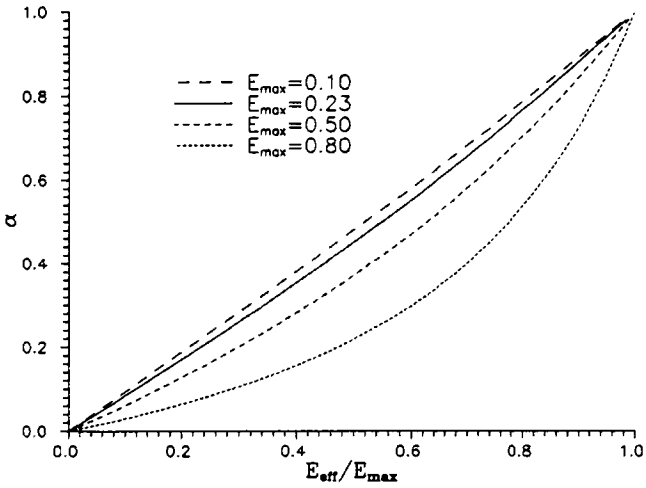

FIGURE 2 Theoretical population of binding extent α in the photobleaching method. α was calculated according to Eq. 11 for $\tau_1 = 1$ s and $\tau_1' = \tau_1/(1 - E_{max})$ for different values of E_{max} as a function of τ_{eff}. E_{eff}/E_{max} was calculated as a function of τ_{eff} too; the graphics show the corresponding values.

within an error range of ±2%. That is

$$\alpha \approx E_{eff}/E_{max}. \quad (12)$$

Binding model

In our system the donors are fluorescein-labeled monoclonal IgE molecules and the acceptor is its specific monovalent hapten. The binding of a hapten, H, to the Fab of an antibody is described by a single binding step. At equilibrium, such a reaction is described by the mass-action law with an intrinsic association constant K_{int}. In binding studies it is often observed that a fraction of the antibodies binding capacity is lost. To account for this we introduce the factor $\beta = [S]/[S]_{tot}$, the mole fraction of functional hapten binding sites, where $[S]_{tot}$ and $[S]$ denote the concentration of the total and functional binding sites, respectively. The expression for the mole fraction α of Fab-hapten complexes follows from the mass conservation and mass-action law:

$$\alpha = \tfrac{1}{2} \cdot [\delta - \sqrt{(\delta^2 - 4[S]_{tot} \cdot \beta \cdot [H]_{tot})}]/([S]_{tot} \cdot \beta) \quad (13a)$$

$$\delta = [S]_{tot} \cdot \beta + [H]_{tot} + K_{int}^{-1}, \quad (13b)$$

where $[H]_{tot}$ denotes the total hapten concentration. In the presence of excess hapten such that $[S]_{tot} \ll [H]_{tot}$, this equation can be simplified to:

$$\alpha \approx [H]_{tot}/(K_{int}^{-1} + [H]_{tot}). \quad (14)$$

In this case α becomes independent of the binding site concentration and presence of antibodies without binding capacity is of no consequence.

MATERIALS AND METHODS

Cell culture

Rat basophilic leukemia cells, subclone 2H3 (RBL-2H3), were cultured at 37°C in Dulbecco's modified Eagle's medium (DMEM) containing 10% fetal calf serum (13).

Labeling of the IgE-antibodies

IgE labeling with FITC (isomer I; Molecular Probes, Eugene, OR) was performed in borate buffer at pH 9.4. The labeled protein was dialysed for 4 d against several 1 liter volumes of phosphate buffered saline (PBS; pH 7.4) to remove unbound dye. The buffer was exchanged every 12 h. The dye/protein ratio was 1.2–2:1. The concentrations of the antibody solutions as well as the labeling ratios were determined by absorption measurements using the following molar extinction coefficients: $\epsilon(IgE)_{280\,nm} = 3 \cdot 10^5\ M^{-1}\ cm^{-1}$ (8), $\epsilon(FITC)_{280\,nm} = 2.7 \cdot 10^4\ M^{-1}\ cm^{-1}$, and $\epsilon(FITC)_{496\,nm} = 8.7 \cdot 10^4\ M^{-1}\ cm^{-1}$.

DNP-haptens

The monovalent *N*-2,4-DNP-ε-amino-*n*-caproic acid (DNP-cap), *N*-2,4-DNP-γ-amino-*n*-butyric acid (DNP-but), and Nε-2,4-DNP-L-lysine (DNP-lys) were obtained commercially from Sigma Chemical Co. (Deisenhofen, Germany) and used without further purification. The concentrations of the DNP stock solutions were determined by absorption measurements using the following molar extinction coefficients: $\epsilon(DNP\text{-}lys)_{364\,nm} = 1.78 \cdot 10^4\ M^{-1}\ cm^{-1}$, $\epsilon(DNP\text{-}cap)_{364\,nm} = 1.77 \cdot 10^4\ M^{-1}\ cm^{-1}$, and $\epsilon(DNP\text{-}but)_{364\,nm} = 1.82 \cdot 10^4\ M^{-1}\ cm^{-1}$.

Preparation of cells for energy transfer experiments

Microscope coverslips (*12 mm diam*) were washed successively in 3% acetic acid, 75% isopropanol, and double distilled water and sterilized by autoclaving. RBL-2H3 cells were grown to subconfluence on the coverslips in DMEM, 10% FCS. For photobleaching experiments at 15° and 25°C the coverslips were washed twice with PBS and incubated with 25 μl of 100 nM FITC-IgE in PBS for 45 min at room temperature. For measurements at 4°C washing and labeling were carried out at 4°C. The coverslips were washed again in PBS before mounting in a small temperature-controlled teflon chamber filled with PBS at 4°, 15°, or 25°C. Cells were allowed to equilibrate in the chamber for 10 min before measurements.

Photobleaching experiments on single cells

Cells attached to coverslips were labeled with fluorescein-IgE and photobleached in a chamber mounted in an epi-illumination fluorescence microscope (Leitz MPV2, Ernst Leitz GmbH, Wetzlar, Germany; see Fig. 3). The fluorescein was excited by the 496.5-nm line (15 mW) of an Argon-ion laser. To gain uniform illumination of the sample the beam was expanded by a beam expander. Irradiation was started by opening a mechanical shutter. Photobleaching was completed within 30 s. The MPV2 is equipped with an image aperture, the

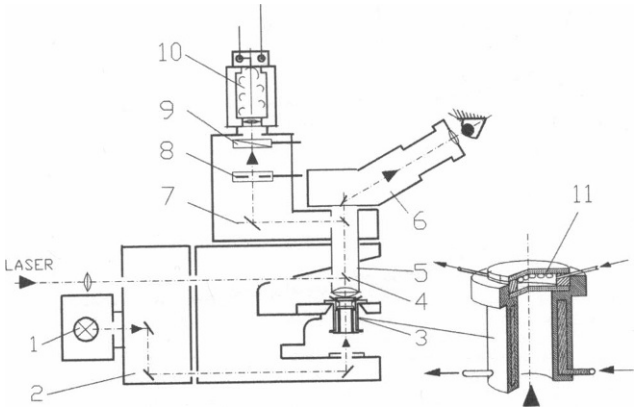

FIGURE 3 Instrument for time-resolved fluorescence measurements on cells. Single cells with receptor bound fluorescein-labeled IgE are selected by visual inspection and photobleached by laser illumination. (1) lamp, (2, 7) mirrors, (3) temperature-controlled teflon chamber, (4) 500 nm dichroic mirror, (6) eyepiece adapter, (8) image aperture, (9) interference filter 515 nm. The time-dependent fluorescence of each cell in the temperature-controlled cell chamber (3, 11) is registered by a photomultiplier (10) with photon counting system.

size of which can be adjusted to the object. This device was used to select single cells for measurements. Fluorescence from an examined cell was focused by a F1 oil immersion 95/1.32 objective and passed through a 500-nm dichroic mirror and a 5-nm HW interference filter centered at 515 nm. The intensity was measured by an Ortec photon counting system (EGΣG Ortec GmbH, Munich, Germany) and the data transferred online to an IBM compatible PC for display and analysis.

Defined amounts of a hapten stock solution were delivered into the chamber. Photobleaching data were then recorded as a function of the DNP-hapten concentration $[H]_{tot}$ in the buffer surrounding the cells. From each coverslip photobleaching data were recorded for at least three different hapten concentrations: $[H]_{tot} = 0$ giving the bleaching time τ_1 for donors alone ($\alpha = 0$); $[H]_{tot}$ in the micromolar range ($\alpha = 1$) giving the bleaching time τ_1', and hapten concentrations in the intermediate range resulting in a set of τ_{eff} values between τ_1 and τ_1' monitoring the mole fraction of haptens bound to the IgE. Each data point was determined using a freshly prepared cover slip. From the thus obtained titration curves the mole fraction α was determined according to Eq. 12. Thus, measurements on several freshly prepared cover slips yielded discrete titration curves $\alpha([H]_T)$. The condition that $[S]_{tot} \ll [H]_{tot}$ was fulfilled for each point of the curve.

Fluorescence titrations of IgE in solution

The binding of DNP-ligands to the FITC-IgE in solution was measured by determining the quenching of both the intrinsic protein tryptophan (14) and the fluorescein emissions. These effects are presumably caused by nonradiative energy transfer to the DNP-groups of the ligands (4, 14). Solution measurements were performed on a MPF-2A Perkin-Elmer Corp. (Norwalk, CT) spectrofluorometer. For tryptophan the excitation wavelength was 280 nm, half width (HW) 4 nm, whereas for FITC the excitation wavelength was 496 nm (HW 2 nm). Tryptophan emission was recorded at 340 nm (HW 6 nm), FITC emission at 520 nm (HW 10 nm). The antibody solution (500 μl) was filled into a temperature-controlled cuvette (4°, 15°, or 25°C) with internal dimensions of 4 × 5 × 35 mm and stirred gently. The hapten solution was added continuously by a stepping motor driven Hamilton Co. (Bonadut, Switzerland) syringe; the hapten addition rate was so slow that the system was in chemical equilibrium at each point of the titration. The data were collected by and stored in a personal IBM compatible computer. Appropriate corrections for dilution and inner filter effects were performed.

In the case of anti-DNP-IgE the intrinsic tryptophan fluorescence with intensity I_0 is quenched to a value I by energy transfer from the tryptophan residues to the DNP of the bound hapten. The quenching $Q = I_0 - I$ is proportional to the mole fraction α of the occupied binding sites and reaches a plateau value Q_{max} at saturation. Hence α is given by:

$$\alpha = Q/Q_{max}. \tag{15}$$

Thus measurement of the tryptophan fluorescence of an IgE solution upon titrating with DNP-haptens allows the determination of α as a function of $[H]_{tot}$. This method cannot be applied to cell bound IgE because the tryptophan emission examined contain contributions from all cellular proteins.

Preparations of cell suspensions for fluorescence titrations

Subconfluent RBL-2H3 cells were released from the culture dishes with 4 mM EDTA in PBS, washed twice in PBS by centrifugation at 4°C, and resuspended to a density of $3 \cdot 10^7$ cells/ml in PBS with added BSA (1 mg/ml). The cells were incubated for 80 min with 100 nm fluorescein-conjugated IgE at 4°C. In this case we used a prolonged incubation time compared with that for the coverslips to ensure saturation of the $Fc_\epsilon RI$ with IgE under the condition of low temperature and higher receptor concentration. The cells were then washed twice with PBS and resuspended to a concentration of 10^7/ml (≈ 5 nM $Fc_\epsilon R$) and were kept at 4°C until transferred to the temperature-controlled cuvette for measurements. Cell viability was checked by trypan blue exclusion after the fluorescence measurements and found to be greater than 95%.

Fluorescence titrations of cell suspension

The binding of DNP ligands to fluorescein-conjugated IgE on cells in suspension was monitored by the extent of emission quenching of the IgE-bound fluorescein. The 496.5 nm line of an Ar-ion laser (Spectra Physics GmbH, Darmstadt, Germany) was used for excitation and emission was registered at 520 nm (HW 3 nm) with a Czerny-Turner double monochromator (Spex GmbH, Munich, Germany) equipped with a photon counting system. The cell suspension was filled into the cuvette described above and was allowed to equilibrate for 15 min at 4°, 15°, or 25°C. The sample was illuminated with an unfocused laser beam (output power 0.2 mW) only during the recording of the fluorescence signal, i.e., for 30 s. The hapten solution was added in discrete amounts with a micropipette. After each addition the solution was mixed carefully with a 100-μl pipette. Thus, a complete titration curve was recorded in ~15 min. Under these conditions no photobleaching of the fluorescein label occurred. For these experiments the concentration of hapten binding sites was in the nanomolar range, so that $[S]_{tot} \approx [H]_{tot}$.

Photobleaching of IgE in solution

Binding isotherms were also determined by photobleaching energy transfer in experiments on fluorescein-conjugated IgE in solution titrated with the DNP haptens. These experiments were in principle carried out in the same way as described for single cells, but with a different experimental setup. Aliquots of PBS with fixed IgE concentration and different DNP-hapten concentrations were filled into 1-mm diam holes in a 1-mm polystyrene plate maintained at 25°C. BSA was added to the solution to avoid adsorption of the IgE on the container walls. The hole was closed from both sides with coverslips creating a chamber which was placed vertically into the path of a ~threefold expanded laser beam (496.5 nm, output power 500 mW). Illumination was started by opening a mechanical shutter and the fluorescence of a very small volume at the center of the sample was imaged onto the entrance slit of a Czerny-Turner double monochromator by a collimator. The fluorescence signal at 520 nm was registered by a photon counting system.

Determination of the equilibrium binding constant K_{int}

Eqs. 13 and 14 are theoretical expressions that give the dependence of α on $[H]_{tot}$, $[S]_{tot}$, K_{int}, and β. Eq. 12 indicates how α is determined experimentally for IgE on single cells as a function of the total hapten concentration $[H]_{tot}$. We employ Eq. 14 to fit these data using K_{int} and E_{max} as fitting parameters. From Eq. 15 the fluorescence titrations of IgE in solution and cell suspension yield the fluorescence intensity I as a function of the total hapten concentration of IgE in solution as:

$$I = I_0 - \alpha \cdot Q_{max}. \quad (16)$$

Hence, by inserting Eq. 13 into Eq. 16 a formalism is derived which can be fitted to the experimental titrations thereby allowing Q_{max}, K_{int}, and β to be free parameters. The photobleaching experiments of IgE in solution were evaluated using Eqs. 12 and 13. To perform all fits we used a χ^2-minimization program named MINUIT from the CERN program library that is described in detail by James (15).

RESULTS

Fluorescence titrations of IgE in solution

We performed fluorescence titrations of the monoclonal IgE-H1-26.82 in solution with three monovalent haptens: DNP-cap, DNP-but, and DNP-lys (Fig. 4). The mole fraction of occupied sites α was determined as a function of the total hapten concentration according to Eq. 15. The mole fraction of active hapten binding sites, β, and the equilibrium binding constant, K_{int}, were calculated by fitting the data. This was done with a computer program that used $[S]_{tot}$, the DNP-stock concentration, and the hapten addition rate as input parameters. The accuracy of the output parameters K_{int} and β obtained by the fitting procedure is limited by the experimental error in determining the input parameters ($\approx 2\%$). This error is emphasized due to the significant correlation between these two parameters as indicated by the χ^2-minimization program Minuit. β was found to be 0.5 ± 0.1; this result was reproducible for several different preparations of IgE-H1-26.82 at all temperatures. The complete results of the titrations at 25°C are summarized in Table 1. The error range given for the different entries of the table is the result of several

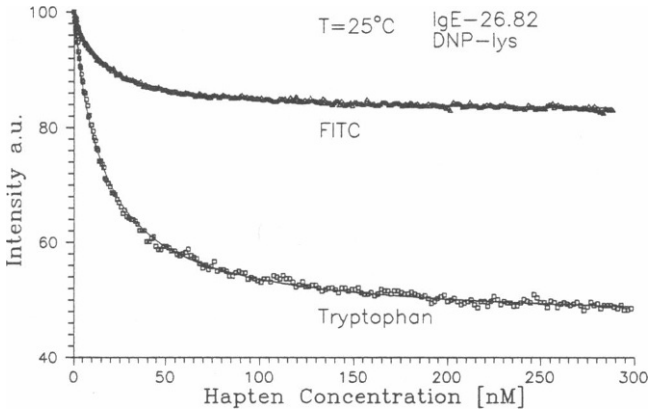

FIGURE 4 Steady state fluorescence of tryptophan residues and of fluorescein (FITC) labels of IgE-H1-26.82 in solution as a function of the added DNP-lys concentration. The data are already corrected for dilution. $[IgE]_{tot}$ = 92 nM for the tryptophan and $[IgE]_{tot}$ = 96 nM for the fluorescein measurement. The solid lines through the data points are the theoretical titration curves. $K_{int} = 6.6 \cdot 10^7\ M^{-1}$, $\beta = 0.47$, $Q_{max} = 52.5\%$ for the tryptophan quenching experiment and $K_{int} = 6.7 \cdot 10^7\ M^{-1}$, $\beta = 0.4$, $Q_{max} = 17\%$ of initial fluorescence for the fluorescein quenching experiment.

TABLE 1 **Equilibrium binding constants and maximum energy transfer efficiencies at saturation of binding sites with the respective haptens at 25°C**

Hapten	Single cells		Solution:	Tryp.	FITC	Cell Suspension
	K_{int} (M^{-1})	E_{max} (%)	K_{int} (M^{-1})	Q_{max} (%)	Q'_{max} (%)	K_{int} (M^{-1})
DNP-cap	$9 \cdot 10^8$	23	$1.2 \cdot 10^8$	49	16	$2 \cdot 10^8$
DNP-lys	$8 \cdot 10^8$	21	$7.1 \cdot 10^7$	52	17	$1.2 \cdot 10^8$
DNP-but	$8 \cdot 10^7$	18	$6.7 \cdot 10^7$	51	17	$1.1 \cdot 10^8$
Error (%)	50	2	10	2	1	30

Q_{max} refers to quenching in solution and suspension experiments, see Eq. 15 and Fig. 4.

repeated titrations. These are the result of the coefficients of variation determined by three to five independent measurements. We performed titrations with both unlabeled and fluorescein-labeled IgE measuring tryptophan quenching. No effect of the label on the equilibrium binding constant K_{int} could be detected and the mole fraction of functional sites β was approximately the same.

To check whether adsorption of IgE on the walls of the cuvette could affect the data, we performed some of the fluorescence titration curves using very low IgE-concentrations ($[IgE]_{tot} < 30$ nM). Within the limit of accuracy, the intrinsic binding constant did not depend on the IgE concentration. Hence adsorption effects were not present.

Photobleaching of fluorescein IgE in solution

We measured the fluorescence decay due to photobleaching for fluorescein-conjugated IgE in solution as a function of the total DNP-lys concentration at 25°C. The decay curves were fitted to single exponentials (data not shown) from which E_{eff} was calculated. Fig. 5 shows the quantity $1 - E_{eff} = \tau_d/\tau_{eff}$, which corresponds to the fluorescence quenching value Q of the FITC-IgE titrations, versus total DNP-ligand concentration. Each data point is the average of 4–8 single measurements (standard error of the mean = 1%). The IgE concentration was adjusted to 11 nM. The solid line was calculated from Eqs. 13 and 16 using the equilibrium binding constant K_{int}, Q_{max}, and β for DNP-lys obtained from the fluorescence quenching titrations. The good agreement between the data and the fluorescence quenching experiments attests to the reliability of results obtained by the photobleaching method.

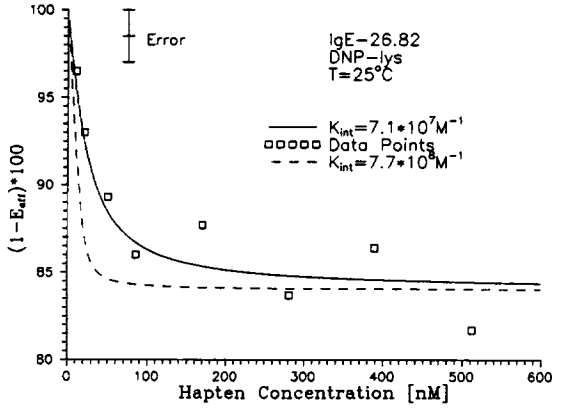

FIGURE 5 The quantity $1 - E_{eff} = \tau_d/\tau_{eff}$ determined by photobleaching of FITC-IgE in solution as a function of total DNP-ligand concentration. $(1 - E_{eff}) \cdot 100$ corresponds to the fluorescence quenching Q of FITC-IgE titrations. Each data point is the average of 4–8 single measurements. The total IgE concentration was 11 nM. The solid and the dashed lines were calculated by Eqs. 13 and 16 using the indicated values of K_{int} and $Q_{max} = 17\%$. β was set to 0.5.

Photobleaching of $Fc_\epsilon RI$-bound IgE on attached cells

We recorded the dependence of the fluorescence bleaching rates of fluorescein conjugated IgE-H1-26.82 and IgE-SPE-7 bound to adherent single RBL-2H3 cells with regard to the total hapten concentration in the surrounding buffer. Fig. 6 shows a typical fluorescence bleaching curve. Such decay curves in general contain two components. One has a large amplitude and a time constant of ~1 s under the particular illumination conditions applied. This component represents the photobleaching of the fluorescein chromophore. The amplitude of the second component was linearly dependent on the aperture size and its bleaching time constant was in the range of 10–20 s. This very small component (~5%) is attributed to the background arising from the coverslip and the immersion oil of the microscope objective. The data were fit by a sum of two exponentials using the χ^2-minimization program MINUIT. Since both the amplitudes and the time constants differed by at least one order of magnitude the potential problems in fitting the sum of exponentials mentioned in Theory were not encountered.

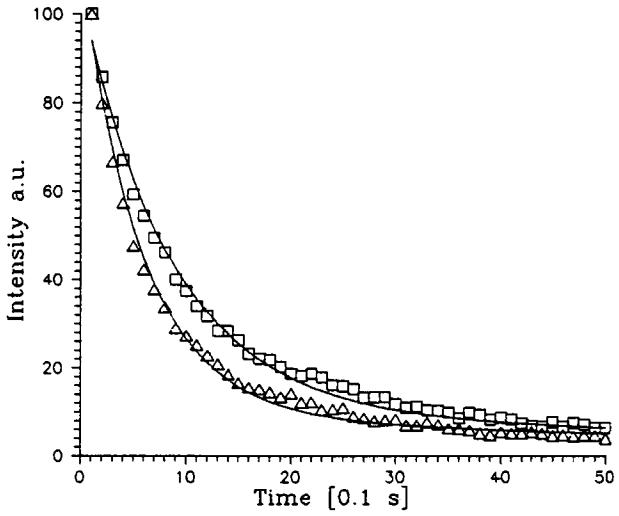

FIGURE 6 Fluorescence bleaching curves of fluorescein-labeled IgE bound to single cells. The small background due to fluorescence of buffer and immersion oil of the microscope objective is already substracted. The full lines are single exponentials fitted to the data. Bleaching of free fluorescein-IgE (△) is faster ($\tau_d = 0.6$ s) than bleaching of the fluorescein-IgE-DNP-lys complex (□: $\tau_s = 0.85$ s). DNP-lys concentration in the chamber was 250 nM.

To obtain the effective bleaching time constant τ_{eff} for a given hapten concentration, 7–15 single cells were bleached and their time constants averaged. The results were found to be independent of cell size and shape. The coefficient of variation of the time constants was in the range of 5–10% and the error of the mean in the range of 1–2%. The averages of τ_{eff} for cells from two different coverslips, however, differed by up to 30%. Thus one obtains a rather large scattering of the observed data (Fig. 7). Repeating this procedure at different hapten concentrations, one obtains the titration curve $\alpha([H]_{tot})$ by virtue of the protocol described under Material and Methods. Fig. 7 displays the titration curves for DNP-but, DNP-cap, and DNP-lys measured at three different temperatures, i.e., T = 25°, 15°, and 4°C.

The concentration of binding sites in the sample chamber can be estimated by determining the number of cells and using the known number of receptors per cell ($3–5 \cdot 10^5$). This yields a $[S]_{tot}$ in the picomolar range. Therefore, for all points of the titration curve, $[S]_{tot} \ll [H]_{tot}$ and Eq. 14 can be used to fit the experimentally obtained titration curves using K_{int} as a free parameter. Thus one derives the solid curves in Fig. 7.

Our solution experiments reveal that only half of the binding sites of the IgE-H1-26.82 samples are active. In this case a combination of bleaching of liganded molecules with time constant τ_1' and of nonfunctional free sites with time constant τ_1 is observed even for saturating hapten concentrations. Therefore, $\tau_{eff,sat}$ depends on β, the mole fraction of functional sites, and is different from τ_1'. However, from $\tau_{eff,sat}$, τ_1 and β it is possible to calculate τ_1' by Eq. 11. One still finds a linear relationship between α and E_{eff} like Eq. 12, where α is related to the total concentration of functional and nonfunctional hapten binding sites. Because β is known one can rescale α to the fraction of functional sites α_f. In the cases of IgE-H1-26.82, with β = 0.5, Eq. 12 holds provided the correct τ_1' is used. In summary, the essential result of this calculation is that the same value for α_f is obtained either assuming ≈50% functional sites and using τ_1' resulting from $\tau_{eff,sat}$ as described above, or assuming 100% functional sites and using $\tau_{eff,sat}$ as τ_1'. This shows that at least for $\beta \geq 0.5$, the results are independent of the fraction of inactive sites.

The standard deviations of the K_{int} values were derived by calculating an upper and lower K_{int} whose corresponding titration curves define an area enclosing 67% of the data points.

The results of the fitting procedure for the measurements at 25°C are summarized in Table 1, the equilibrium binding constants for all three temperatures are given in Table 2. The given error for K_{int} is the range of K_{int} values describing 67% of the data points within their individual error ranges. The maximal energy transfer efficiency $E_{max} = 1 - \tau_1/\tau_1'$ at saturation of the cell bound IgE with hapten was ~22% for DNP-cap and DNP-lys, but only 18% for DNP-but. For the first two haptens this is higher than the corresponding values for IgE in solution obtained by the quenching of the fluorescein emission of IgE in solution upon addition of saturating concentrations of DNP haptens. This produces a value of 16–17% as shown in Table 1.

Comparison of the derived K_{int} values in Table 2 *a* for cell-bound IgE and in solution shows that IgE-H1-26.82 exhibits a higher affinity toward DNP-cap and DNP-lys when bound to the cell surface than free in solution. Here again DNP-but shows a different behavior. For DNP-but the equilibrium binding constant is equal in both situations.

To illustrate the difference between the intrinsic affinity of free and (attached) cell-bound IgE for the binding of DNP-cap and DNP-lys, we calculated the corresponding titration curves for the K_{int}-values describing the binding to IgE in solution (Table 2, second column). This yields the dashed lines in Fig. 7. It is apparent that their deviations from the best fit cannot be explained in terms of statistical errors in spite of the large scattering of the data.

As a control for our results with IgE-H1-26.82 we performed similar measurements on a different DNP-specific, monoclonal IgE produced by a different hybridoma clone, i.e., SPE-7. As in the case of the 26.82 IgE, a quenching of the emission of conjugated fluorescein is observed, albeit with a higher efficiency (E_{max} = 23% for FITC-IgE-SPE-7 using DNP-cap in solution). The mole fraction of functional binding sites, β = 0.7, was higher than for IgE-H1-26.82, but K_{int} was somewhat smaller ($3 \pm 1 \cdot 10^7$ M^{-1}). Titration with the same hapten of IgE bound to adherent, single cells resulted in a $K_{int} = 1 \pm 0.5 \cdot 10^8$ M^{-1}, again a value higher than that for IgE in solution. The results are listed in Table 2 *b*.

Fluorescence titrations of $Fc_\epsilon RI$ bound IgE on cells in suspensions

The dependence of fluorescence quenching on the total concentration of the three haptens for fluorescein-conjugated IgE-H1-26.82 bound to cells in suspension was determined as described above. The data analysis was performed in the same way as that for the IgE in solution. In contrast to the IgE-solution measurements, the concentration of binding sites could only be estimated. Hence we treated it as a free parameter and used the data to derive $\beta \cdot [S]_{tot}$ in Eq. 13. The direct correlation between the concentration of binding sites

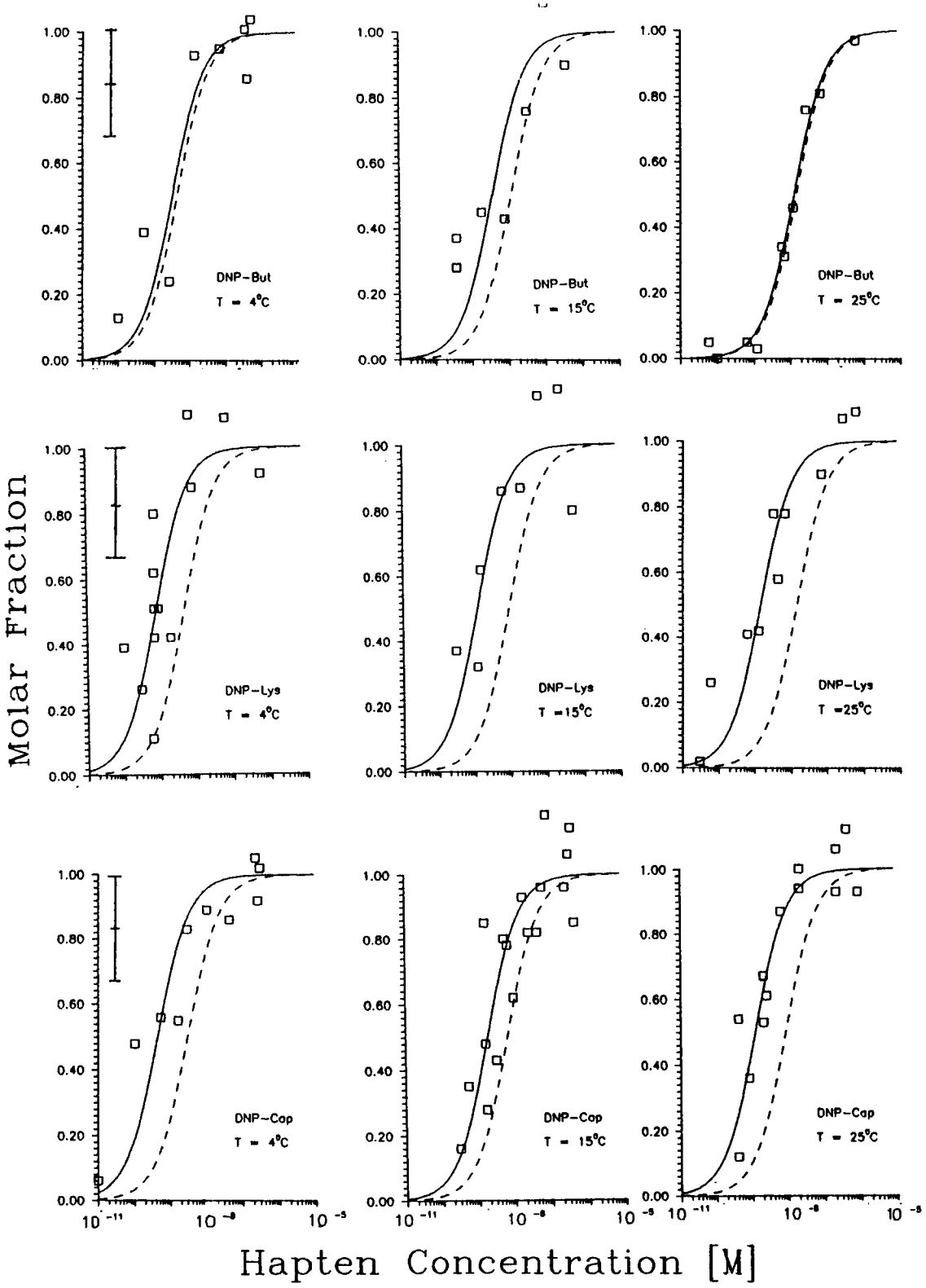

FIGURE 7 Mole fraction α of occupied binding sites on the surface of single cells as a function of hapten concentration. Cells were sensitized with fluorescein-labeled IgE-H1-26.82 bound to Fc_ϵ receptors. Each data point represents an average over 7–15 single cells. Solid lines are fits according to Eq. 14. The dashed lines are calculated using the respective K_{int}-values for the binding to free IgE in solution. The bar to the left of the titrations indicates the error range.

TABLE 2 **Equilibrium binding constants for binding isotherms at 4°, 15°, and 25°C for the respective haptens binding to IgE-H1-26.82 and IgE-SPE-7 in solution, bound to cells in suspension and to live single cells**

K_{int} $10^7 M^{-1}$	Solution	Cell suspension	Single cell
(*a*) Hybridoma clone H1-26.82			
4°C			
DNP-cap	35 ± 3	37 ± 12	248 ± 100
DNP-lys	22 ± 2	22 ± 7	117 ± 50
DNP-but	23 ± 2	18 ± 7	20 ± 10
15°C			
DNP-cap	16 ± 2	14 ± 5	56 ± 30
DNP-lys	11 ± 2	16 ± 6	103 ± 50
DNP-but	9 ± 2	15 ± 5	29 ± 15
25°C			
DNP-cap	12 ± 4	19 ± 6	94 ± 40
DNP-lys	7 ± 2	12 ± 6	77 ± 30
DNP-but	7 ± 2	11 ± 4	8 ± 15
(*b*) Hybridoma clone SPE-7			
25°C			
DNP-cap	3 ± 1	—	10 ± 5

and K_{int} mentioned above limit the accuracy of the K_{int} determination, especially in this analysis where we had considerably fewer data points for each titration curve as compared with the fluorescence titrations of IgE in solution. The results of the data analysis are summarized in Tables 1 and 2. The errors are coefficients of variation deduced from two to four single individual measurements. Despite the large uncertainties one can state that the results of suspension measurements agree well with those derived from the solution studies.

DISCUSSION

Resonance energy transfer measurements on single attached cells by the photobleaching method yield a transfer efficiency E of ~18–23% for fluorescein-labeled IgE-H1-26.82 upon saturation with DNP-haptens bound to the type I Fc_ϵ-receptors on living RBL-2H3 cells. From the measurements carried out at 25°C we derived the equilibrium binding constants $K_{int} = 9 \cdot 10^8$, $8 \cdot 10^8$, and $8 \cdot 10^7$ M^{-1} for the monovalent haptens DNP-cap, DNP-lys, and DNP-but, respectively. These results illustrate the feasibility of performing quantitative binding isotherms on single, adherent, living cells.

Our control experiments, photobleaching of IgE in homogenous solutions, yield results identical to those of well-established fluorescence titrations (4). This supports the reliability of the method and the data analysis. Further corroboration is the fact that the extent of energy transfer attained at saturation of the binding sites with hapten is identical for cell suspension and single cell measurements, i.e., $E_{max} \approx 22\%$. As Table 2 shows, the binding constants of DNP-cap and DNP-lys to $Fc_\epsilon RI$ bound IgE were found to be ~4–11 times higher than those for binding of these haptens to free IgE in solution. This finding is unexpected because we, as well as Erickson et al. (4), find the same binding constants by measurements in solution and on cells in suspension. Hence our data indicate that IgE-H1-26.82 bound to adherent single cells behaves differently than when bound to cells in suspension. That is, it exhibits an apparently higher affinity for some ligands. Moreover a similar effect is observed for the binding of DNP-cap to IgE-SPE-7. This suggests that the observed effect is not unique for the IgE-H1-26.82.

One potential critique of the analysis of the titration curves is that fluorophores bound to targets on the surface of cells may exhibit broad distributions of exponential decay rates (16). To check whether this can affect the linear relationship between the molar fraction α and the corresponding effective time constant τ_{eff}, the following protocol was employed:

(*a*) First we assumed that the apparent photobleaching decay rates $k'_1 = 1/\tau'_1$ exhibit a homogeneous distribution. In a normalized form it is given by:

$$f(k'_1) = \begin{cases} 1/(k'_{1,u} - k'_{1,l}) & \text{for } k'_1 \in [k'_{1,u}, k'_{1,l}] \\ 0 & \text{for } k'_1 \notin [k'_{1,u}, k'_{1,l}] \end{cases}, \quad (17)$$

where $k'_{1,u}$ and $k'_{1,l}$ denote the upper and lower limit of the interval considered.

The fraction $g^*(t)$ of donors in the excited state can now be formulated by means of the Laplace transform of $f(k'_1)$:

$$g^*(t) = \int_0^\infty g_0^* f(k'_1) e^{-k'_1 t} : e^{-k'_1 t}\, dk'_1. \quad (18)$$

The fluorescence intensity $F(t)$ is derived by evaluating the integral. By regarding the second exponential of the bleaching curves as a constant background F_B, it can be written as:

$$F(t) = \frac{F_0(e^{-k'_{1,u}t} - e^{-k'_{1,l}t})}{(k'_{1,l} - k'_{1,u})t} + F_B, \quad (19)$$

where F_0 is the initial fluorescence intensity at $t = 0$.

(*b*) This equation was used to generate a bleaching curve assuming a distribution interval of $k'_{1,l} = 1.2\ s^{-1}$ and $k'_{1,u} = 2.4\ s^{-1}$.

This bleaching curve was exactly reproduced by fitting to a monoexponential function with $k'_{1,eff} = 1.75\ s^{-1}$. The distribution interval was then increased until a monoexponential fit failed. This occurred for $k_{1,l} < 0.6\ s^{-1}$ and

$k_{2,1} > 3.0\ s^{-1}$. Because all bleaching curves evaluated in this study can be fitted in terms of a monoexponential decay, we conclude that for the time regime of the bleaching process (cf. Fig. 6), the upper limit of the distribution width was $2.4\ s^{-1}$ corresponding to the above cited limit. The corresponding effective decay rate is $1.6\ s^{-1}$.

(*c*) In a third step we assume that the decay rate distribution is shifted to lower rates by a factor of 0.8 owing to energy transfer to an adjacent acceptor. Thus the effective decay rate is lowered to $1.28\ s^{-1}$. This corresponds to an energy transfer efficiency of 20%. By fitting the respective bleaching curve, one derives an effective decay rate of $k_{1,eff} = 1.27\ s^{-1}$, from which an energy transfer efficiency of 19.9% was calculated. This clearly shows that the effective decay rates can be used to calculate the correct energy transfer efficiency.

(*d*) To check whether in our binding experiments the effective decay rate is linearly related to the molar fraction α of bound haptens, we have generated bleaching curves for different α by using the homogenous decay rate distributions introduced above. These decay curves were fitted to monoexponential functions. The corresponding effective decay rates were still found to depend linearly on the molar fraction.

These model calculations establish that the titration curves shown in Fig. 7 can be evaluated by means of Eq. 12 even if one assumes that the decay rates exhibit a quite broad distribution due to spatial and structural heterogeneities of the target. This confirms the difference in affinities for ligand binding to adherent–cell-bound IgE. A satisfactory explanation of this phenomenon, however, is not yet available.

In conclusion, the determination of energy transfer by photobleaching of individual cells is advantageous over measurements of cell suspensions because (*a*) corrections for spectral overlap are avoided; (*b*) photobleaching during data acquisition is not a problem; (*c*) a fluorescent acceptor is not required; and (*d*) the cells are at least perturbed from their adherent state. This means that the perturbation of sensitive cell systems is as small as possible. For cells that cannot be cultured and can only be obtained in small numbers this method of measuring energy transfer may be the only one applicable. Further, since each single cell is inspected visually by a microscope it is easy to exclude dead or damaged cells. The photobleaching method can be applied in a fluorescence microscope, it is using arc-lamp or laser excitation. A digital imaging system or a photon counting system is used for the registration of the emission signal. The digital imaging system (6, 7, 11) has the advantage of high spatial resolution in the cell yet requires relatively expensive hardware components. The measurement with a photomultiplier lacks the option of spatial resolution but is a cheap, sensitive, and rapid measuring device. Instruments for measuring fluorescence recovery after photobleaching (FRAP) can readily be adapted for energy transfer measurements.

In this first quantitative application we made an interesting observation: monoclonal, DNP-specific IgE molecules display a virtual higher affinity toward its specific hapten when it is bound to the surface of attached cells than when it is bound to released cells in suspension or when it is free in solution.

We gratefully acknowledge many stimulating discussions with Dr. D. J. Arndt-Jovin, as well as her help concerning experimental details. We would like to thank Prof. Schloot and his group (FB 2, University of Bremen) for lab space and assistance with the cell culture as well as Prof. Boseck for supply of the Leitz MPV2; Mr. Lasch and Mr. Ankele for technical assistance. We thank Mr. Ankele for drawing Figs. 1 and 2 with AUTOCAD.

Support of the research work reported here has been generously provided by grants from The Fritz Thyssen Foundation, F.R.G. and from The Council for Tobacco Research-USA Inc. U. Kubitscheck gratefully acknowledges a fellowship from the "Studienstiftung des Deutschen Volkes."

Received for publication 19 September 1990 and in final form 2 April 1991.

REFERENCES

1. Metzger, H., G. Alcaraz, R. Hohman, J.-P. Kinet, V. Priluda, and R. Quarto. 1986. The receptor with high affinity for immunoglobulin E. *Annu. Rev. Immunol.* 4:419–470.
2. Ortega, E., R. Schweitzer-Stenner, and I. Pecht. 1988. Possible orientational constraints determine secretory signals induced by aggregation of IgE receptors on mast cells. *EMBO (Eur. Mol. Biol. Organ.) J.* 7:4101–4109.
3. Schweitzer-Stenner, R., A. Licht, I. Lüscher, and I. Pecht. 1987. Oligomerization and ring closure of immunoglobulin E class antibodies by divalent haptens. *Biochemistry.* 26:3602–3612.
4. Erickson, J., P. Kane, B. Goldstein, D. Holowka, and B. Baird. 1986. Cross-linking of IgE-receptor complexes at the cell surface: a fluorescence method for studying the binding of monovalent and bivalent haptens to IgE. *Mol. Immunol.* 23:769–781.
5. Kane, M. P., D. Holowka, and B. Baird. 1988. Cross-linking of IgE-receptor complexes by rigid bivalent antigens >200 Å in length triggers cellular degranulation. *J. Cell Biol.* 107:969–980.
6. Jovin, T. M., and D. J. Arndt-Jovin. 1989. FRET microscopy: digital imaging of fluorescence resonance energy transfer. Application in cell biology. *In* Cell Structure and Function by Microspectrofluorometry. E. Kohen, J. S. Ploem, and J. G. Hirschberg, editors. Academic Press, Orlando, FL. 99–117.
7. Jovin, T. M., and D. J. Arndt-Jovin. 1989. Luminescence Digital Imaging Microscopy. *Annu. Rev. Biophys. Biophys. Chem.* 18:271–308.
8. Liu, F. T., J. W. Bohn, E. L. Ferry, H. Yamamoto, C. A. Molinaro, L. A. Sherman, N. R. Klinman, and D. H. Katz. 1980. Mono-

clonal dinitrophenyl-specific murine IgE antibody: preparation, isolation, and characterization. *J. Immunol.* 124:2728–2736.

9. Eshhar, Z., M. Ofarim, and T. Waks. 1980. Generation of hybridomas secreting murine reaginic antibodies of anti-DNP specificity. *J. Immunol.* 124(2):775–780.
10. Förster, T. 1948. Zwischenmolekulare Energiewanderung und Fluoreszenz. *Ann. Physik.* 2:55–75.
11. Jovin, T. M., D. J. Arndt-Jovin, G. Marriott, R. M. Clegg, M. Robert-Nicoud, and T. Schormann. 1990. Distance, wavelength and time: the versatile 3rd dimensions in light emission microscopy. *In* Optical Microscopy for Biology. B. Herman, and K. Jacobsen, editors. Wiley-Liss, Inc. 575–602.
12. Grinvald, A., and I. Z. Steinberg. 1974. On the analysis of fluorescence decay kinetics by the method of least-squares. *Anal. Biochem.* 59:583–598.
13. Barsumian, E. L., C. Isersky, M. G. Petrino, and R. P. Siraganian. 1981. IgE induces histamine release from rat basophilic leukemia cell lines: isolation of releasing and nonreleasing clones. *Eur. J. Immunol.* 11:317–323.
14. Archer, G. A., T. C. McGuire, and H. Krakauer. 1973. Interpretation of fluorescence quenching titrations of antihapten antibody having overlapping hapten quenching domains. *Biochemistry.* 12:2151–2155.
15. James, F. 1972. Function minimization. *Proc. CERN-Computing Data Processing School, Pertisau/Austria.* 72–121.
16. Benson, D., J. Bryan, A. L. Plant, A. M. Gotto, Jr., and L. C. Smith. 1985. Digital imaging fluorescence microscopy: spatial heterogenity of photobleaching rate constants in individual cells. *J. Cell Biol.* 100:1309–1323.